Photoinduced Transient Stark Spectroscopy in Organic Semiconductors: A Method for Charge Mobility Determination in the Picosecond Regime

J. Cabanillas-Gonzalez, T. Virgili, A. Gambetta, and G. Lanzani
IFN-CNR, Dipartimento di Fisica, ULTRAS-INFM-CNR, Politecnico di Milano, Milano 20133, Italy

T. D. Anthopoulos
Blackett Laboratory, Department of Physics, Imperial College London, London SW7 2BW, United Kingdom

D. M. de Leeuw
Philips Research Laboratories, Professor Holstlaan 4 (WAG 11), 5656 AA Eindhoven, The Netherlands
(Received 13 October 2005; published 13 March 2006)

Subpicosecond photoinduced Stark spectroscopy experiments are carried out for measuring charge carrier mobility in organic semiconductors. The technique is demonstrated in state-of-art devices based on methanofullerene. The transient mobility of photogenerated charge carriers is measured in the picosecond time domain. Electric field dependent mobility is observed from the earliest time scales. In addition, two distinct transport regimes are revealed: a short-lived state, approximately 10 ps, of high mobility and a transient towards the trap limited transport, associated with the mesoscopic structure of the medium.

DOI: 10.1103/PhysRevLett.96.106601 PACS numbers: 72.80.Rj, 72.80.Ng, 78.47.+p, 78.66.Tr

Charge carrier mobility in organic semiconductors is a critical material property that determines the performance characteristics of many electronic devices, including field-effect transistors [1], light-emitting diodes [2], and solar cells [3]. For this reason, many experimental techniques and theoretical modeling have been devoted to its measure and interpretation [4–7]. It turns out that different experiments provide different values of carrier mobility in the same material, due to varying experimental conditions and different device architectures. For instance, it is found that the hole mobility of common polymer semiconductors is several orders of magnitude lower when tested in light-emitting diodes than in field-effect transistors [8,9]. Such variations make material evaluation difficult if not impossible.

In amorphous organic materials charge carrier mobility is often the average of a number of slowing down processes where defects and traps dominate. Ideally one would like to measure the carrier mobility in a pure, defect free material, so meaningful comparison between different experiments and theory would be allowed. Close to this ideal case is the use of time resolved microwave conductivity technique, an electrodeless method that monitors charge dipoles absorption in the transient regime [7,10]. The time resolution of this technique is limited, however, to the nanosecond domain. Here we present an alternative approach, based on photoinduced transient Stark effect in which optical probing is exploited for extracting mobility values in the picosecond time regime. A related technique, exploiting the Franz-Keldysh effect in extended band states, was successfully employed by Shank *et al.* to measure nonequilibrium carrier transport in inorganic semiconductors [11–13]. The validity of our method relies on the fact that charge transport is monitored *in situ* on the compound without current extraction, avoiding pitfalls caused by carrier migration along macroscopic regions of the sample as well as by carrier extraction at semiconductor-metal electrode interfaces. Mobilities obtained in this way can be considered as upper limit values, unaffected by limiting processes such as trapping or recombination. This information is intrinsic and constitutes a direct feedback for the design of new materials with improved properties.

In this work we report on the experimental determination of the charge carrier mobility in [6, 6]-Phenyl C_{61}-butyric acid methyl ester (PCBM) in the picosecond time range. This soluble methanofullerene is of particular interest in organic optoelectronics due to its high carrier mobility and attractive processing properties [14–16]. Our approach consists of monitoring changes in the ground state electroabsorption (EA) during the process of charge separation. PCBM exhibits a strong Stark feature centered at 2.3 eV. Following photogeneration in a PCBM diode under reverse bias, singlets are separated into electron-hole pairs. These charge pairs act as *dipoles* leading to a *photoinduced polarization* opposed to the applied field [17]. As they drift farther apart their associated dipole moment increases and the electric field inside the illuminated area is gradually screened as reflected by a 75% reduction of the Stark feature. By monitoring the EA during the first 40 ps we infer the evolution in the average *e*-h separation as well as charge mobility values.

PCBM devices were prepared from a 60 g/l chlorobenzene solution of PCBM with 0.7% weight content of polystyrene spin coated at 1600 rpm on polyethylenedioxythiophene coated indium-tin-oxide substrates. Typical film thicknesses were in the range of 113–120 nm. Finally, gold electrodes were deposited on top of the film by thermal evaporation in high vacuum (10^{-6} mbar). Conventional pump-probe measurements [18] were carried out in unbiased devices placed in vacuum (10^{-3} mbar),

 © 2006 The American Physical Society

exciting with 3.2 eV, 180 fs pulses and an excitation density of 0.35 mJ cm^{-2}. The measurements yield the differential transmission $\Delta T/T$ as a function of pump-probe delay (τ) and probe energy (ω):

$$\Delta T/T(\omega, \tau) = -d\sum_{i,j}\sigma_{ij}(\omega)\Delta N_J(\tau) \otimes f_p, \qquad (1)$$

where d is the film thickness, σ_{ij} the cross section for $j \rightarrow i$ transition, ΔN_j the pump induced change in the j-state population, and f_p the normalized probe pulse temporal profile. For electric field assisted pump-probe measurements, [see Fig. 1(a)], 500 Hz square profile electric fields ranging from 0.6 to 1.5 MV/cm were applied across the devices in reverse configuration to minimize charge injection. The obtained signal corresponds to the field induced changes on $\Delta T/T$ given by $(\Delta T/T)_F - \Delta T/T = \Delta T^2/T$. Following Eq. (1),

$$\Delta^2 T/T = -d\sum_{i,j}\Delta\sigma_{ij}(\omega, F)\Delta N_J \otimes f_p - d\sum_{i,j}\sigma_{ij}(\omega)\Delta^2 N_J(F) \otimes f_p - \sum_i \Delta\sigma_{i0}(F)N_0, \qquad (2)$$

where the first term on the right- hand side is the Stark shift of the excited state transition, the second term represents the field induced change in the population of excited states, and the last term is the Stark shift of the ground state transition. Since the ground state population N_0 is virtually pump independent, and hence time independent, the EA contribution is often a flat background. In our case, however, we will show that the electric field inside the sample is time dependent, thus introducing kinetics in the EA term.

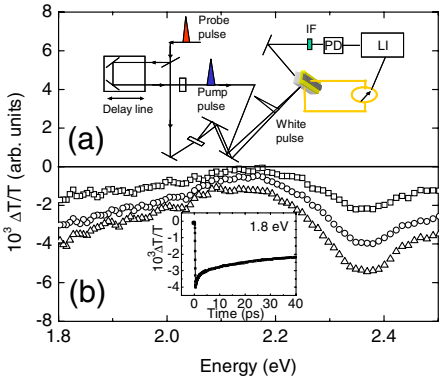


FIG. 1 (color online). (a) Electric field assisted pump-probe setup. Single wavelength detection is provided by the combination of interforemeter filters (IF), photodiode (PD), and lock-in amplifier (LI) referred to in the ac field. The electric field is modulated at 500 Hz, i.e., the pulse repetition rate. This configuration leads to only one pump-probe arrival within the on/off regime. (b) Differential transmission spectra at 4 (triangles), 40 (circles), and 200 ps (squares) pump-probe delay. The spectra exhibit two PA bands. The PA dynamics at 1.8 eV are shown in the inset.

Figure 1(b) displays $\Delta T/T$ spectra at different pump-probe delays characterized by photoinduced absorption (PA) bands located at 2.4 and 1.8 eV. These features are observed in C_{60} solid films too and assigned to excited state absorption from the lowest singlet excited state ($S_1 - S_n$) [19]. Proof for this common origin is the equal reduction in PA signal detected in both spectral locations when changing the pump-probe delay from 4 to 200 ps. PA dynamics [Fig. 1(b), inset] fit to a stretched exponential with a decay rate of $8.3 \times 10^{-3} \times t^{-0.4}$ ps^{-1}. The initial fast component could be attributed to bimolecular singlet-singlet annihilation, its investigation being beyond the scope of this work. The steady state (CW)-EA spectrum (Fig. 2) shows a peak centered at 2.3 eV, typical of unsubstituted fullerenes [19], and assigned to Stark shift of the $S_0 - S_2$ transition. At negative pump-probe delays (pump follows probe), the $\Delta^2 T/T$ spectra show a clear resemblance with the CW-EA spectrum because the ground state EA term [see Eq. (2)] is the only non-null contribution. At positive pump-probe delays the $\Delta^2 T/T$ spectrum does not change in shape but shows a dramatic 40% reduction at 1 ps delay, which evolves towards 75% after 20 ps, (Fig. 2, inset). Hereby, the $\Delta^2 T/T$ signal is composed of both Stark shift of the $S_0 - S_2$ *absorption* and field induced change in $S_1 - S_n$ PA. The predominant contribution is, however, the change in ground state EA following photoexcitation, as inferred from the following: (i) The effect of the electric field on $\Delta T/T$ (40%–75% reduction) is significantly larger than the signal ascribed to $S_1 - S_n$ quenching from S_1 ionization ($\sim$ 10%) [20]. (ii) S_1 ionization should manifest as a positive contribution to $\Delta^2 T/T$, due to reduced PA, which would yield to an over all enhancement of $\Delta^2 T/T$, opposite to the observed quenching. (iii) $\Delta^2 T/T$ at 1.8 eV (region of negligible ground state EA) shows much faster time resolved formation (see inset of Fig. 2). Here the signal is composed of a positive step rise which differs

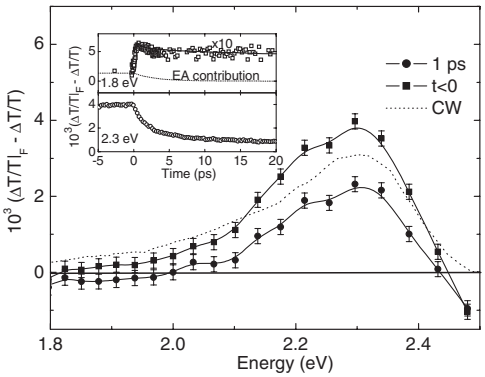


FIG. 2. Electric field pump-probe spectra at different delay times (straight line). A CW-EA spectrum (dashed line) is shown for comparison purposes. The inset depicts the electric field pump-probe dynamics at 2.3 eV (open circles) and 1.8 eV (open squares) with its EA contribution (dotted line). $\Delta T/T$ dynamics at 1.8 eV (bold line) are plotted normalized to $\Delta^2 T/T$ for comparison purposes. Note that both follow the same trend.

from the gradual decrease observed at 2.3 eV. This represents the true $\Delta^2 N$ contribution from singlet ionization (S_1 population reduction) and suggest that singlets are being dissociated mainly within the pulse duration. Although a similar ultrafast dissociation mechanism has been demonstrated in poly(9-9 dioctylfluorene) (PFO) [21], this behavior is not present in all conjugated polymers. In methyl ladder-type poly(para-phenylene), for instance, gradual dissociation evolves within the exciton lifetime [22,23]. A similar dissociation mechanism has also been reported in PFO oligomers [24]. (iv) There is a perfect correlation between the $\Delta^2 T/T$ spectrum and the EA spectrum.

All this suggests that the internal field is modified by the presence of the pump induced charged pairs. These pairs, acting like dipoles, will have a preferential orientation opposed to the polarity of the applied electric field. Owing to this new photoinduced polarization, the applied field is partially screened, giving rise to a decrease in the EA signal as predicted by the quadratic dependence on field amplitude. We should now consider two important points. First, singlet dissociation is almost completed beyond the pulse duration [see point (iii) above]. Such an impulsive singlet dissociation, which was observed previously in other materials such as PFO [21], rules out gradual charge generation as responsible for the slow EA quenching. Second, also charge recombination is negligible within 20 ps since both $\Delta^2 T/T$ and $\Delta T/T$ at 1.8 eV follow parallel trends, suggesting that the percentage of photogenerated charges does not change substantially within the first 20 ps (inset of Fig. 2). We can then conclude that the photoinduced charge population in the device is stationary during our time window, so that the time resolved decrease of the EA signal must be attributed to *evolution* of the photoinduced polarization. This effect is caused by the drift of electrons and holes towards the countersign electrodes, therefore increasing the modulus of each photogenerated dipole. Note that we discard any influence of charge accumulation on the kinetics since the latter effect would be independent of the pump-probe delay. Moreover, charge accumulation should not be significant according to the 2 ms field on-off period and the 115 nm thickness of the film which facilitates efficient charge collection. The evolution of the EA signal up to 40 ps under different fields is shown in Fig. 3. The inset displays the field dependence of the onset values found at negative delays, showing a good agreement with the quadratic dependence predicted for EA. From the fit parameters, we obtain a time dependent effective electric field given by $F_{\mathrm{eff}}(t) \approx [\mathrm{EA}(t)/0.0013]^{1/2}$.

The average drift induced electron-hole separation distance [25], $\langle R \rangle$ can be calculated as $\varepsilon_o[F_{\mathrm{app}} - F_{\mathrm{eff}}(t)]/eN_p$, where F_{app} and N_p hold, respectively, for the applied electric field and the density of photogenerated pairs. The latter can be estimated from the reduction in singlet population, which according to Eq. (2) is given by $\Delta^2 N \approx [\Delta^2 T/T - \Delta\sigma_{S1-Sn}(F)N_0]/\sigma_{S1-Sn}d$. From the initial $\Delta^2 T/T$ value at 1.8 eV, the ground state EA contribution and the $S_1 - S_n$ absorption cross section (σ_{S1-Sn}) of 1.17×10^{-17} cm^2, we obtain $N_p \approx 4.6 \times 10^{18}$ cm^{-3}, leading therefore to a 13% quantum yield for charge photogeneration [26]. Accordingly, the temporal evolution of $\langle R \rangle$ is displayed in Fig. 4. The maximum values for $\langle R \rangle$ range from 1 to 4 nm reached after 40 ps. Note that since the size of a PCBM molecule comprises 1 nm and the average hopping distance is estimated as 3.4 nm [27], the lower $\langle R \rangle$ values we report correspond to charge motion inside a crystalline monodomain or even a single molecule.

The charge carrier mobility (μ) can be extracted from $\frac{d\langle R(t)\rangle}{dt}/F_{\mathrm{eff}}(t)$ where the result is attributed to the more mobile charge when measured in unipolar transport materials. In the case of PCBM, however, calculated μ might correspond to either electron or holes since recent reports showed that both are equally mobile [14,28]. Figure 5 shows the evolution of mobility with time and electric field, with early values ranging from 0.05 to 0.2 cm^2/V s for the highest applied fields. According to this figure we can distinguish two regimes of transport: (i) an early regime weakly time dependent, where μ is described by

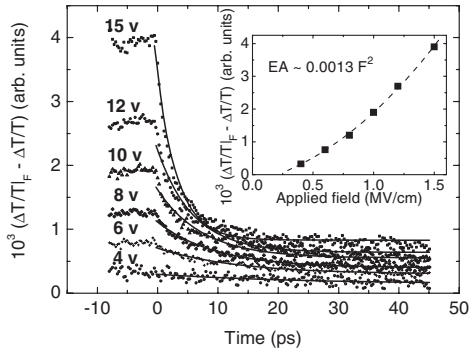


FIG. 3. Electric field pump-probe dynamics under different fields. Dynamics were fitted to a single exponential law with fairly good agreement producing lifetimes which range between 3 to 25 ps when fields evolve from 1.5 to 0.4 MV/cm. The dependence of the electroabsorption signal at negative time values on the applied field follows a quadratic law (inset).

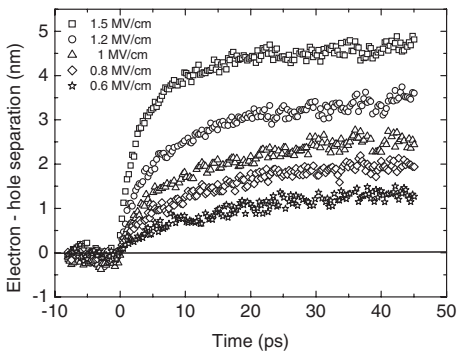


FIG. 4. Evolution of the electron-hole separation under 1.5 (squares), 1.2 (circles), 1 (triangles), 0.8 (diamonds), and 0.6 MV/cm (stars) during the first 40 ps after photoexcitation.

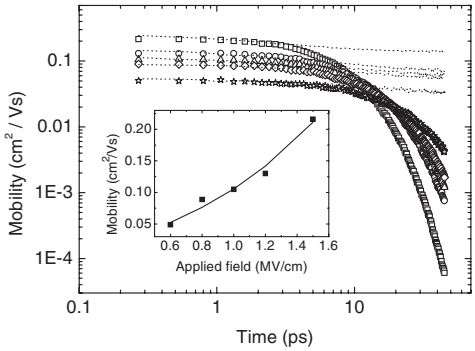


FIG. 5. Electron mobility values under 1.5 (squares), 1.2 (circles), 1 (triangles), 0.8 (diamonds), and 0.6 MV/cm applied fields (stars) during the first 40 ps after photoexcitation. The dotted lines hold for the values predicted by the Poole-Frenkel expression given by $\mu(t) = \mu_0 \exp[\gamma\sqrt{F(t)}]$, with μ_0 and γ being the zero-field mobility and the field activation coefficient, respectively. Both parameters are determined from the early mobility values measured at different fields (inset). Accordingly, μ_0 amounts to 4.8×10^{-3} $cm^2/V\,s$ and γ to 3×10^{-3} $(V/cm)^{-1/2}$. Discrepancies between experimental and theoretical values are manifested at long time scales.

the Poole-Frenkel field dependence, and (ii) a highly dispersive transport regime. Owing to the small value of $\langle R \rangle$ the initial behavior might correspond to transport within short-range crystalline domains where the charge pairs are photogenerated. This hypothesis is supported by the comparable electron mobilities found in C_{60} single crystals (0.5 $cm^2/V\,s$) [29] and C_{60} based transistors [30]. The dispersive regime is characterized by a dramatic mobility decrease. The latter cannot be ascribed exclusively to either screening of the applied field, attending to clear deviation from the Poole-Frenkel model (Fig. 5), or charge recombination (negligible during the first 20 ps). Moreover, the larger the applied field is, the earlier mobility collapses. Hereby, the more likely scenario is fast carrier drift towards interdomain boundaries where trapping becomes effective and contributes to a slow down of the carriers. The farther the carriers travel, the faster and more efficiently they get trapped. This could account for the strong mobility quenching at 1.5 MV/cm. In this case the mobility falls after only 4 ps corresponding to an $\langle R \rangle$ of 3 nm, i.e., approximately the average length of one single hop.

In conclusion, we demonstrate that electric field assisted pump-probe experiments allows direct determination of carrier mobilities in the picosecond time domain in organic semiconductors. The technique exploits the Stark shift of the molecular transition and the partial screening caused by the photoinduced charges. We found at early times that carrier mobility in PCBM films is very high, comparable to single crystal values. Transition to a slower transport regime occurs on time scales essentially determined by the characteristic length scale of the medium.

J. C.-G. acknowledges financial support from the EC under Project No. HPRN-CT-2002-00327 (EUROFET).

[1] C. D. Dimitrakopoulos and P. R. L. Malenfant, Adv. Mater. **14**, 99 (2002).
[2] R. H. Friend *et al.*, Nature (London) **397**, 121 (1999).
[3] J. Nakamura, K. Murata, and K. Takahashi, Appl. Phys. Lett. **87**, 132105 (2005).
[4] H. Bässler, Phys. Status Solidi B **175**, 15 (1993).
[5] Gilles Horowitz, Adv. Mater. **10**, 365 (1998).
[6] M. C. J. M. Vissenberg and M. Matters, Phys. Rev. B **57**, 12 964 (1998).
[7] J. M. Warman and M. P. de Haas, *Pulse Radiolysis*, edited by Y. Tabata (CRC, Boca Raton, FL, 1991), Chap. 6.
[8] C. Tanase *et al.*, Phys. Rev. Lett. **91**, 216601 (2003).
[9] C. Tanase, P. W. M. Blom, and D. M. de Leeuw, Phys. Rev. B **70**, 193202 (2004).
[10] R. J. O. M. Hoofman *et al.*, Nature (London) **54**, 54 (1998).
[11] C. V. Shank and D. H. Auston, Science **215**, 797 (1982).
[12] C. V. Shank *et al.*, Appl. Phys. Lett. **38**, 104 (1981).
[13] E. A. Schiff *et al.*, Appl. Phys. Lett. **54**, 1911 (1989).
[14] T. D. Anthopoulos *et al.*, Adv. Mater. **16**, 2174 (2004).
[15] T. D. Anthopoulos *et al.*, Appl. Phys. Lett. **85**, 4205 (2004).
[16] H. Hoppe and N. S. Sariciftci, J. Mater. Res. **19**, 1924 (2004).
[17] V. Gulbinas *et al.*, Phys. Rev. B **66**, 233203 (2002).
[18] G. Lanzani *et al.*, Phys. Status Solidi **201**, 1116 (2004).
[19] D. Dick *et al.*, Phys. Rev. Lett. **73**, 2760 (1994).
[20] T. Virgili *et al.*, in "Photophysics of Molecular Materials," edited by G. Lanzani (Wiley-VCH, New York, to be published).
[21] T. Virgili *et al.*, Phys. Rev. Lett. **90**, 247402 (2003).
[22] V. Gulbinas *et al.*, Phys. Rev. Lett. **89**, 107401 (2002).
[23] W. Graupner *et al.*, Phys. Rev. Lett. **81**, 3259 (1998).
[24] J. Cabanillas-Gonzalez *et al.*, Phys. Rev. B **71**, 155207 (2005).
[25] $\langle R(t) \rangle$ represents the increase in e-h separation due to the drift of the carriers in the applied field with respect to the initial one in the nascent charge transfer state.
[26] σ_{S1-Sn} was calculated as $\Delta T/T/(N_s \times d)$, with $\Delta T/T$ the initial differential transmission value at 1.8 eV, d the PCBM film thickness (115 nm) and N_s the initial singlet population of 3.1×10^{19} estimated from the pump fluence (0.35 $mJ\,cm^{-2}$) and the absorbance of the PCBM fim (0.7).
[27] V. D. Mihailetchi *et al.*, Adv. Funct. Mater. **13**, 43 (2003).
[28] S. M. Tuladhar *et al.*, Adv. Funct. Mater. **15**, 1171 (2005).
[29] E. Frankevich, Y. Maruyama, and H. Ogata, Chem. Phys. Lett. **214**, 39 (1993).
[30] T. B. Singh *et al.*, Org. Electron. **6**, 105 (2005).